Two-Dimensional Simulation of Subcritical Flow at a Combining Junction: Luxury or Necessity?

Rabih Ghostine[1]; Robert Mose[2]; José Vazquez[3]; Abdellah Ghenaim[4]; and Caroline Grégoire[5]

Abstract: Classically, in open-channel networks, the flow is numerically approximated by the one-dimensional Saint Venant equations coupled with a junction model. In this study, a comparison between the one-dimensional (1D) and two-dimensional (2D) numerical simulations of subcritical flow in open-channel networks is presented and completely described allowing for a full comprehension of the modeling of water flow. For the 1D, the mathematical model used is the 1D Saint Venant equations to find the solution in branches. For junction, various models based on momentum or energy conservation have been developed to relate the flow variables at the junction. These models are of empirical nature due to certain parameters given by experimental results and moreover they often present a reduced field of validity. In contrast, for the 2D simulation, the junction is discretized into triangular cells and we simply apply the 2D Saint Venant equations, which are solved by a second-order finite-volume method. In order to give an answer to the question of luxury or necessity of the 2D approach, the 1D and 2D numerical results for steady flow are compared to existing experimental data.

DOI: 10.1061/(ASCE)HY.1943-7900.0000230

CE Database subject headings: Open channels; Critical flow; Steady flow; Flow.

Author keywords: Saint Venant equations; Open channels.

Introduction

In the design of flood control channels, one of the most important hydraulic problems is the analysis of the flow conditions at open-channel junctions. Typical examples of these junctions are encountered in urban water networks, irrigation and drainage canals, and natural river systems. Many problems in water resources, river mechanics, and environmental hydraulics require accurate description of the characteristic parameters of the flow regime in these open-channel networks.

An open-channel network system may consist of a number of interconnected river branches joined at a number of junctions. For a one-dimensional (1D) model, the presence of internal junctions poses difficulties in numerical solution of unsteady flow through the system because these junctions act as internal boundary conditions for each channel joined at a junction (Yen 1979). The values of the flow parameters (stage and velocity) at these internal nodes are a function of the solution, which vary with time. Therefore, 1D flow simulation in open-channel networks is much more complicated than single channel solutions, especially for large-scale networks (Akan and Yen 1981; Yen and Osman 1976). The whole system is considered as a set of branches in which the 1D Saint Venant equations are applied and linked by different junction models. The hydraulic conditions at a junction can be modeled by the mass conservation equation and either the energy conservation equation or the momentum equation. Different combining junction models exist in the literature and are of empirical nature as certain model parameters are based on experimental results and hence their range of validity may be limited. The simplest junction model is the equality of water stage model, which is used by most of applications in the hydraulic engineering. More recent models were proposed by Gurram et al. (1997), Hsu et al. (1998a,b), and Shabayek et al. (2002).

In this work, we simulate and compare results of a 1D model with those obtained from the two-dimensional (2D) Saint Venant equations in the case of subcritical flow. The 1D Saint Venant equations are coupled with the Shabayek et al. (2002) model to find the solution in the network system. For the 2D case, the whole system (branches and junction) is considered as one system and discretized into triangular cells forming an unstructured computational mesh, and the 2D Saint Venant equations are solved by a second-order finite-volume method. The study is focused on the prediction of the water depths at the junction. The obtained results for subcritical steady flow through combining junctions are shown and compared to existing experimental results obtained by different authors. The objective of this paper is to show that the 1D approximation is not acceptable in all cases and that with a classical 2D approach, we can obtain very accurate results with a reasonable space discretization and therefore a reasonable CPU time.

Literature Review

Previous studies on combining subcritical open-channel flows proposed theoretical approaches based on the mass and momen-

[1]Doctor, IMFS, UMR 7507, UDS-ENGEES-CNRS, Strasbourg, France (corresponding author). E-mail: rabih.ghostine@engees.u-strasbg.fr

[2]Professor, IMFS, UMR 7507, UDS-ENGEES-CNRS, Strasbourg, France. E-mail: rmose@imfs.u-strasbg.fr

[3]Professor, IMFS, UMR 7507, UDS-ENGEES-CNRS, Strasbourg, France. E-mail: jvazquez@engees.u-strasbg.fr

[4]Professor, INSA, Laboratoire de Génie de la Conception, Strasbourg, France. E-mail: abdellah.ghenaim@insa-strasbourg.fr

[5]Professor, LHYGES, UMR 7517, UDS-ENGEES-CNRS, Strasbourg, France. E-mail: caroline.gregoire@engees.u-strasbg.fr

Note. This manuscript was submitted on September 11, 2007; approved on March 19, 2010; published online on March 27, 2010. Discussion period open until March 1, 2011; separate discussions must be submitted for individual papers. This technical note is part of the ***Journal of Hydraulic Engineering***, Vol. 136, No. 10, October 1, 2010. ©ASCE, ISSN 0733-9429/2010/10-799–805/$25.00.

tum conservation for determining the upstream-to-downstream depth ratio. Taylor (1944) presented the first study on junction flow and referred to the complexity of the problem. He conducted experiments in horizontal rectangular channels of junction angles of 45° and 135°. For a given downstream flow depth h_d and upstream-to-downstream discharge ratio $q_u=Q_u/Q_d$, he derived an equation for the relative upstream flow depth $Y_u=h_u/h_d$. A comparison with data showed fair agreement for $\delta=45°$ and poor agreement for $\delta=135°$.

A second systematic study on junction flow was presented by Webber and Greated (1966). A small model with junction angles $\delta=30°$, $\delta=60°$, and $\delta=90°$ was used. Modi et al. (1981) investigated open-channel junction using conformal mapping and therefore did not take into account energy losses. Best and Reid (1984) analyzed experimentally the geometry of the separation zone at sharp-edged open-channel junctions. Based on the experimental approach of Best and Reid (1984), Hager (1987) introduced a simple model in which the pressure distribution on the lateral sidewall and the lateral momentum contribution were taken into account. He aimed at predicting the width of the separation zone by a 1D approach. Ramamurthy et al. (1988) studied combining open-channel flow at a right-angled junction based on the momentum transfer from the lateral to main branch. He applied separate momentum equations for the flow in the lateral and main channels. The lateral momentum contribution was found to increase as the lateral discharge ratio increases.

Gurram et al. (1997) studied the characteristics of the lateral flow and the flow contraction in the tailwater channel and determined expressions for the momentum correction coefficient and the lateral wall pressure force. An equation for the ratio of flow depths in the lateral and upstream branches was also provided. Hsu et al. (1998a,b) applied overall mass and energy conservations to the junction and momentum conservation to two control volumes in the junction and computed an energy loss coefficient and the depth ratio. All of the above-noted studies were for equal-width junction flows and equality of the upstream flow depths was assumed. Recently, Shabayek et al. (2002) developed a 1D model providing the necessary internal boundary equations for combining subcritical open-channel junctions. The advantage of this model is that it does not assume equal upstream flow depths. The model is based on the momentum principle together with mass continuity through the junction. Shabayek et al. (2002) used an analytical approach for solving the upstream-to-downstream depth ratio Y_u and the lateral-to-downstream depth ratio Y_L.

1D Study

For the 1D simulation, the 1D Saint Venant equations are applied in branches while these equations are not applicable within the junction which is treated as an internal boundary condition. Junction models or conditions are generally empirical and so are limited to the conditions under which they were developed, for example, subcritical flow and for a network system composed of three rectangular branches linked by one combining junction.

1D Combining Junction Model

Consider a network system composed of three rectangular branches linked by one combining junction. We denote by branch u, branch L, and branch d the main channel located upstream of the junction, the lateral channel branching to the main channel, and the main channel located downstream of the junction, respectively (see Fig. 1). The water depths and discharges at the upstream, lateral, and downstream points to the junction are denoted by h_u, h_L, h_d, Q_u, Q_L, and Q_d. The junction angle is denoted by δ.

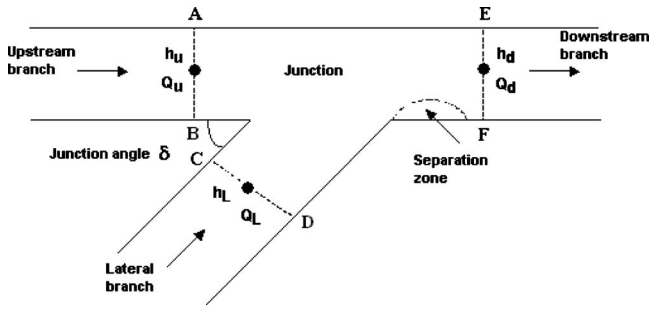

Fig. 1. 1D junction problem

The recent model of Shabayek et al. (2002) which is quite general was selected for this study. It does not assume the equality of water stages, or the equality of widths, and apply the momentum principle in the streamwise direction to two control volumes in the junction together with overall mass conservation. The equations derived by Shabayek et al. (2002) are

$$q_u-\frac{q_u^2}{w_1Y_u}-\frac{1}{8F_d^2}[w_1(3Y_u^2-2Y_uY_L-Y_L^2)+q_u(Y_u^2+2Y_uY_L+Y_L^2-4)]-\frac{1}{2F_d^2}\left(\frac{L_1S_0}{h_d}\right)(w_1Y_u+q_u)+K^*\left(\left[\frac{q_u}{w_1Y_u}\right]^2-\left[\frac{q_L}{w_2Y_L}\right]^2\right)\times(Y_u+Y_L)[2q_Lq_u]+\frac{L_1}{B_dC_*^2}\left(1+\frac{B_d}{h_d}q_u\right)=0 \quad (1a)$$

$$q_L-\frac{q_L^2}{w_2Y_L}-\frac{1}{8F_d^2}[w_2(3Y_L^2-2Y_uY_L-Y_u^2)+q_L(Y_L^2+2Y_uY_L+Y_u^2-4)]-\frac{1}{2F_d^2}\left(\frac{L_2S_0}{h_d}\right)(w_2Y_L+q_L)-K^*\left(\left[\frac{q_u}{w_1Y_u}\right]^2-\left[\frac{q_L}{w_2Y_L}\right]^2\right)\times(Y_u+Y_L)[2q_Lq_u]+\frac{L_2}{B_dC_*^2}\left(1+\frac{B_d}{h_d}q_L\right)+K\frac{q_L^3}{w_2^2Y_L}=0 \quad (1b)$$

where $q_u=Q_u/Q_d$ and $q_L=Q_L/Q_d=1-q_u$=upstream-to-downstream and the lateral-to-downstream discharge ratios, respectively, and $F_d^2=Q_d^2/(gb_d^2h_d^3)$=Froude number at the beginning of the downstream branch. B_u, B_L, and B_d=widths in upstream, lateral, and downstream branches of the junction. $w_1=B_u/B_d$ and $w_2=B_L/B_d$=upstream-to-downstream and lateral-to-downstream width ratios. S_0=longitudinal slope of the junction. C_*=Chezy nondimensional coefficient and L_1 and L_2=outer lengths of the two control volumes. K^*=interfacial shear coefficient and K=separation zone coefficient. According to Shabayek et al. (2002), the values of K^* and K are given by $K^*=-0.0015\delta+0.3$ and $K=0.0092\delta-0.1855$.

Coupling the Channel Solution with the Junction Solution

The solution at the internal points enclosing the junction involves six unknowns variables, h_d, Q_d, h_L, Q_L, h_u, Q_u, and so six equations are needed to solve the 1D junction problem. Three equations are derived from the branches' solutions through the characteristics equations

$$\begin{cases} Q_u = f_u(h_u) \\ Q_L = f_L(h_L) \\ Q_d = f_d(h_d) \end{cases} \quad (2)$$

For more details about the method of characteristics, see Garcia-Navarro and Saviron (1992). One corresponds to the conservation of mass at the junction

$$Q_u + Q_L = Q_d \quad (3)$$

The last two equations are derived from Shabayek et al. (2002) model [Eqs. (1*a*) and (1*b*)]. The system of these six equations is nonlinear and its solution is obtained by a Newton-Raphson method.

2D Study

2D Saint Venant equations

The 2D depth integrated shallow water equations are obtained by integrating the Navier-Stokes equations over the flow depth with the following assumptions: uniform velocity distribution in the vertical direction, incompressible fluid, hydrostatic pressure distribution, and small bottom slope. The continuity and momentum equations are

$$\frac{\partial U}{\partial t} + \frac{\partial E}{\partial x} + \frac{\partial G}{\partial y} = S \quad (4)$$

in which

$$U = \begin{pmatrix} h \\ hu \\ hv \end{pmatrix}, \quad E = \begin{pmatrix} hu \\ hu^2 + gh^2/2 \\ huv \end{pmatrix}, \quad G = \begin{pmatrix} hv \\ huv \\ hv^2 + gh^2/2 \end{pmatrix}$$

and

$$S = S_0 + S_f = \begin{pmatrix} 0 \\ ghS_{0x} \\ ghS_{0y} \end{pmatrix} + \begin{pmatrix} 0 \\ -ghS_{fx} \\ -ghS_{fy} \end{pmatrix} \text{ is the source term}$$

where u and v=velocity components in the x and y directions, respectively; h=water depth; g=acceleration due to gravity; (S_{0x}, S_{0y})=bed slopes in the x and y directions; and (S_{fx}, S_{fy})=friction slopes in the x and y directions, respectively. In this study, the friction slopes are estimated by using Manning's formula

$$S_{fx} = \frac{n_M^2 u\sqrt{u^2+v^2}}{h^{4/3}}, \quad S_{fy} = \frac{n_M^2 v\sqrt{u^2+v^2}}{h^{4/3}}$$

where n_M=Manning's roughness coefficient.

Numerical Method

A cell-centered finite-volume method is formulated for Eq. (4) over a triangular control volume, where the dependent variables of the system are stored at the center of the cell and represented as piecewise constants. Integrating Eq. (4) over the area of the ith control volume, one obtains

$$\int_{A_i} \frac{\partial U}{\partial t} dA + \int_{A_i} \nabla \cdot F dA = \int_{A_i} S dA \quad (5)$$

where $F = E\vec{i} + \vec{G}$ and A_i=area of the control volume.

Using the divergence theorem, the second integral on the left-hand side of Eq. (5) can be replaced by a line integral around the control volume

$$\int_{A_i} \frac{\partial U}{\partial t} dA + \int_{\Gamma_i} F \cdot n d\Gamma = \int_{A_i} S dA \quad (6)$$

where Γ_i=boundary of the ith control volume and n=unit outward vector normal to the boundary. Approximating the line integral by a midpoint quadrature rule, Eq. (6) can be written as

$$\frac{dU_i}{dt} = -\frac{1}{A_i}\sum_{j=1}^{3} F^* \cdot n_{ij} \Delta\Gamma_{ij} + S_i \quad (7)$$

where i and j denote the ith cell and the jth edge of the cell, respectively; U_i and S_i are the average quantities stored at the center of the ith cell; n_{ij}=unit outward normal vector at the jth edge; $\Delta\Gamma_{ij}$=length of the jth edge; and $F^*=F^*(U_L, U_R)$=numerical flux through the edge which is computed by an exact or approximate Riemann solver. U_L and U_R are the reconstructions of U on the right and the left of an edge.

The present model employs the Roe (1981) Riemann solver to compute the normal flux at the face of a control volume. To obtain a second-order scheme in space, we use the monotone upstream-centered schemes for conservation laws approach for the reconstruction of U_L and U_R at the interfaces [for more details, see Frazao and Guinot (2007) indeed of Guinot (2007)].

Time Integration

The second-order accurate two-stage TVD Runge-Kutta scheme of Cockburn and Shu (1998) is employed in this work. Denoting the right-hand side of Eq. (7) as $L(U)$, an optimal second-order TVD Runge-Kutta method is given by

$$U^{(1)} = U^n + dt \cdot L(U^n)$$

$$U^{n+1} = \frac{1}{2}[U^n + U^{(1)} + dt \cdot L(U^{(1)})] \quad (8)$$

Since The TVD Runge-Kutta method is an explicit scheme, the time step dt must be selected based on the Courant-Friedrich-Lewy stability criterion. The maximum allowable time step is limited in this paper by the following:

$$dt = \text{CFL}\frac{A_i}{\sum_j \Delta\Gamma_{ij} \min(u \cdot n_x + v \cdot n_y - c, 0)} \quad (9)$$

where $0 < \text{CFL} \leq 1$=Courant number.

Boundary Conditions

Boundary conditions are imposed at the face of the cell and the values of the conserved variables at the face are extrapolated from the cell center. According to the theory of characteristics (Hirsch 1990), the Riemann invariants of the 1D shallow water equations are

$$R^- = u + 2c, \quad R^+ = u - 2c \quad (10)$$

which are conserved along $dx/dt = u + c$ and $dx/dt = u - c$, respectively, when the contributions of the source terms are neglected. R^- and R^+ denote the states to the right and left of a face, respectively, and $c = \sqrt{gh}$ is the wave celerity. Since the right side of a boundary is outside the domain, the R^- condition is replaced by

Table 1. Experimental Details for Previous Experimental Studies

Author date	Taylor (1944)	Webber and Greated (1966)	Gurram (1994)	Hsu et al. (1998a,b)
B_u, B_L, B_d (nm)	101.6	127	500	155
q_u	0.4, 0.6, 0.8	0.2, 0.4, 0.5, 0.6, 0.8	0.25, 0.5, 0.75	0.08–0.91
δ	45°, 135°	30°, 60°, 90°	30°, 60°, 90°	30°, 45°, 60°, 90°
F_d	0.20–0.75	0.20–0.60	0.25, 0.5, 0.75, 1	0.57–0.91

the boundary condition itself. For 2D shallow water equations, the R^+ condition is given as

$$(u,v)_L \cdot n + 2\sqrt{gh_L} = (u,v)_* \cdot n + 2\sqrt{gh_*} \tag{11}$$

where the subscripts * and L denote the variables at the boundary and the left side, respectively. Eq. (11) is combined with the boundary condition to compute the normal flux at the boundary. The normal flux at the boundary is given as

$$F^* \cdot n = \begin{pmatrix} h_*(u,v)_* \cdot n \\ h_* u_* (u,v)_* \cdot n + \frac{1}{2} g h_*^2 n_x \\ h_* v_* (u,v)_* \cdot n + \frac{1}{2} g h_*^2 n_y \end{pmatrix} \tag{12}$$

where n_x and n_y=components of n in the x and y directions, respectively.

According to the theory of characteristics (Hirsch 1990), two boundary conditions are needed when the flow regime is subcritical. For a subcritical flow, a boundary condition is imposed in the form of flow depth, unit discharge, or velocity. In the case of a depth boundary condition, h_* is given and $(u,v)_* \cdot n$ is computed directly from Eq. (11). In the case of a velocity boundary condition, $(u,v)_* \cdot n$ is given and h_* is computed by modifying Eq. (11). Finally, the normal flux in Eq. (12) can be computed by using h_*, u_*, and v_*.

A free slip condition is applied at the solid boundary, i.e., the normal velocity component at the face is set to zero

$$(u,v)_* \cdot n = 0 \tag{13}$$

and h_* is computed by using Eq. (11).

Numerical Results and Discussion

The experimental observations of Taylor (1944), Webber and Greated (1966), Gurram (1994), and Hsu et al. (1998a,b) are used for a preliminary models verification of the prediction of water depth. Fig. 1 shows the geometric configuration of the junctions considered in the studies of Taylor (1944), Webber and Greated (1966), Gurram (1994), and Hsu et al. (1998a,b). In these studies, the flow was subcritical throughout and the branches were horizontal, rectangular of equal width. In all these studies, the measurements used for the comparison were taken at the three cross sections near the junction (AB, CD, and EF) shown in Fig. 1. These sections are located between two and four times the width of the channel.

For the numerical simulation, the boundary conditions are given as follows: for a known upstream flow discharge Q_u, a known lateral flow discharge Q_L, and a known downstream water depth h_d, the depth ratios Y_u and Y_L are computed using the 1D approach and the 2D Saint Venant equations. The Manning roughness coefficient is fixed to zero. Table 1 shows the experimental details for the different experimental studies. For the 1D simulation, each branch was discretized into 20 cells while for the 2D simulation, the computational domain (branches and junction) was triangulated into 1,290 cells (Fig. 2).

Experimental Setup of Hsu et al. (1998a,b)

In their study, the flows upstream of the main and branch channels were subcritical and values of the downstream Froude number were taken in the range of $0.57 < F_d < 0.91$. The experiments were carried out in a rectangular flume made of plywood with a horizontal bed. The main and branch flumes were 12 and 4 m long, respectively. Both flumes were 0.155 m wide with junction angles, δ, being 30°, 45°, 60°, and 90°. The junction corners were sharp-edged in order to reduce the friction effects of the flume boundaries.

Figs. 3 and 4 present the variation of the measured and the computed depth ratios Y_u and Y_L, respectively, for δ=30°, 45°, 60°, and 90°. For δ=30°, the 1D approach gives acceptable results and very good agreement between the 2D Saint Venant equations and the experimental data is obtained. For δ=45°, the results obtained by the 2D Saint Venant equations are also very close to the experimental data but a remarkable difference is found between the 1D approach and the experiments. The discrepancy between the 1D approach and the experimental data increases also for the two angles of 60° and 90° and becomes more serious, while the 2D results agree well with the experimental data and very good agreement is still found.

For a more quantitative assessment of the water depth ratios' prediction Y_u and Y_L, we introduce an estimator of quality E_Y as follows:

$$E_Y = 100 \cdot \max \left| \frac{Y_p - Y_m}{Y_m} \right| \tag{14}$$

where Y_p and Y_m=predicted and measured depth ratios, respectively. Table 2 shows values of E_Y for the 1D and the 2D ap-

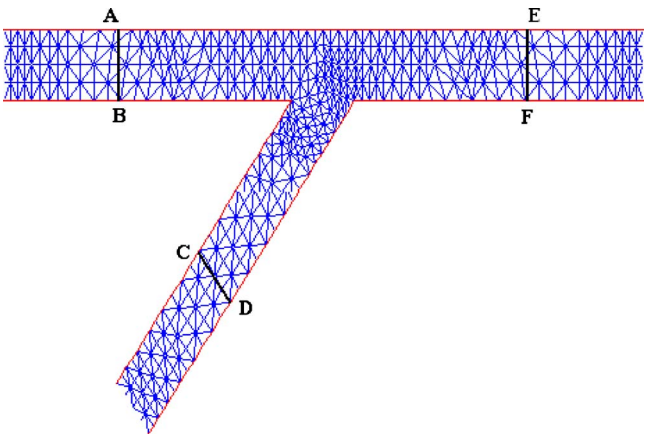

Fig. 2. Unstructured mesh of the junction

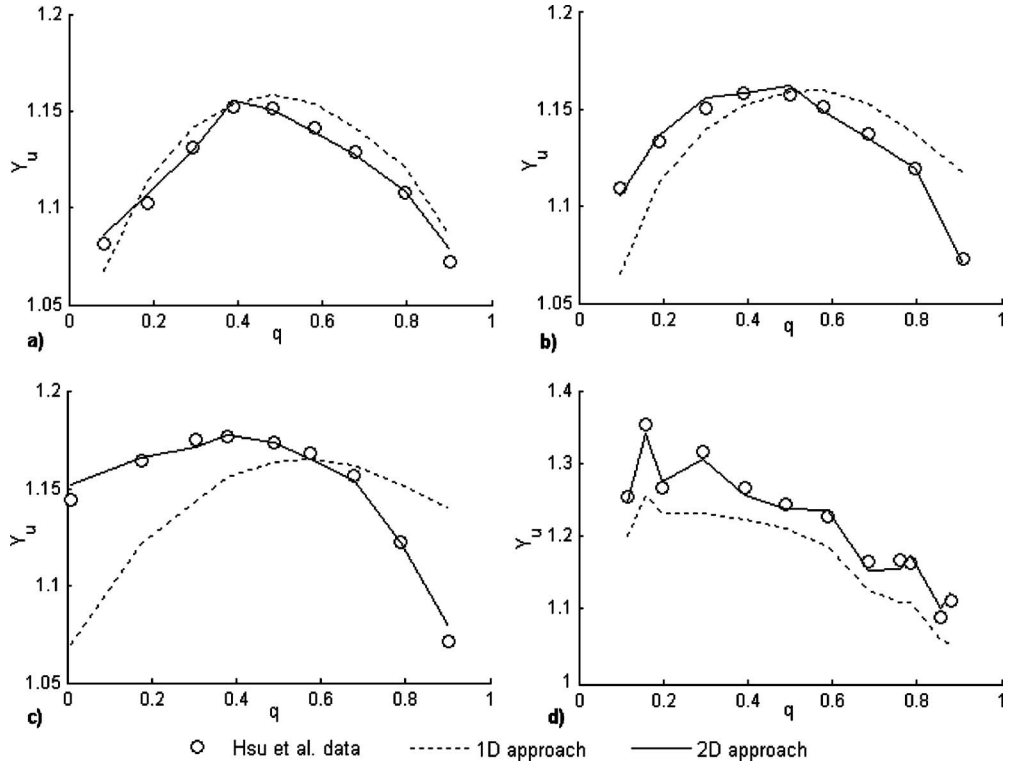

Fig. 3. Comparison of the main channel depth ratios with the data of Hsu et al. (1998a,b): (a) angle 30°; (b) angle 45°; (c) angle 60°; and (d) angle 90°

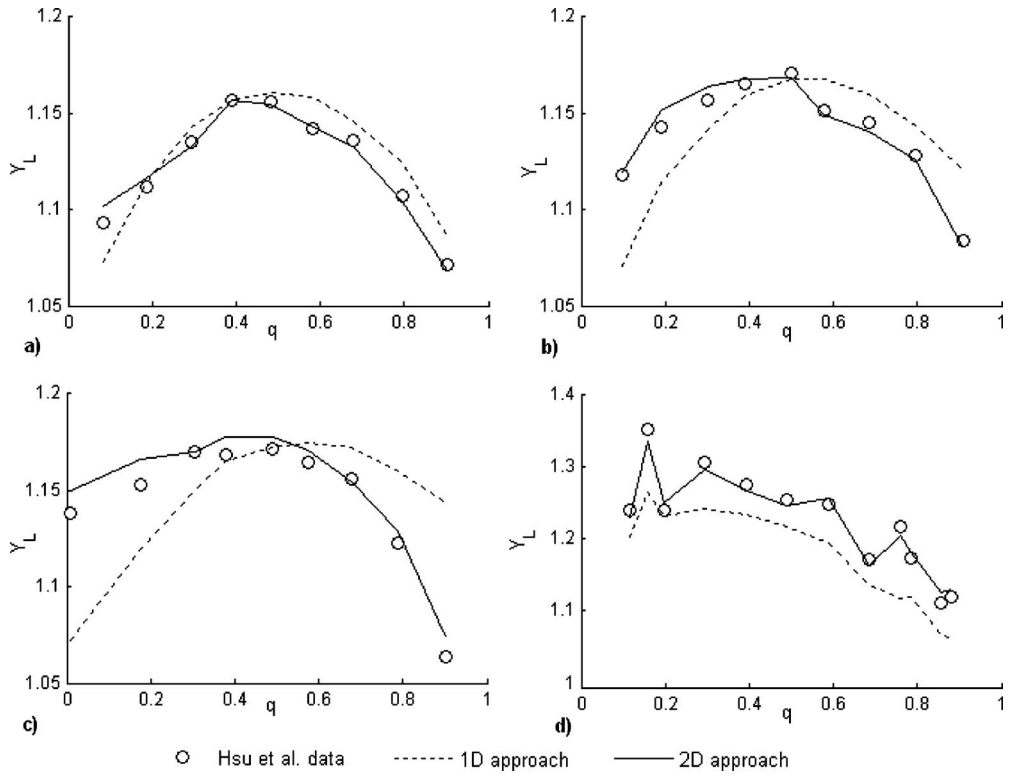

Fig. 4. Comparison of the lateral branch depth ratios with the data of Hsu et al. (1998a,b): (a) angle 30°; (b) angle 45°; (c) angle 60°; and (d) angle 90°

Table 2. Percentage Error [according to Eq. (14)] for the Two Approaches (1D and 2D) with respect to the Data of Hsu et al. (1998a,b)

Angle	E_{Y_u} (1D)	E_{Y_u} (2D)	E_{Y_L} (1D)	E_{Y_L} (2D)
30°	1.32	0.62	1.81	0.79
45°	4.17	0.45	4.26	0.75
60°	6.51	0.64	7.55	0.99
90°	7.26	0.91	8.18	1.26

proaches. In all the investigated tests, the 2D approach gives the best agreement with the experimental data with $E_Y < 1\%$ in all cases. For the 1D approach, the error is acceptable for the angle of 30° but it increases with the junction angle and reaches 8.18% for the angle of 90°.

Other Experimental Data

Webber and Greated (1966) and Gurram (1994) presented their results in the form of plots of the main channel depth ratio, Y_u, versus the downstream Froude number, F_d, for the different discharge ratios, q_u, and the different junction angles, δ. Taylor (1944) plotted Y_u versus a lateral channel kineticity coefficient which can be related to F_d and q_u. Fig. 5 compares the experimental data with the two approaches 1D and 2D for different discharge ratios and junction angles.

According to Fig. 5, the experimental results are correctly reproduced by the 2D approach. The figure indicates a good agreement between the experimental data and the results obtained by the 2D approach. This approach correlates well to the measured data and gives better accuracy than the ones provided by the 1D approach, which does not always achieve a very good agreement. We can find good agreement between the 1D approach and the experimental data for small values of F_d. Once F_d increases, the discrepancy between the 1D approach and the experimental data increases and becomes more critical.

Conclusions

In this study, a comparison between the 1D and the 2D simulations of subcritical flow through combining junctions is presented. For the 1D study, the 1D Saint Venant equations coupled with Shabayek et al. (2002) junction model are used to find the solution in the network system (branches and junction), while for the 2D case, the whole system is discretized into triangular cells forming an unstructured computational mesh and the 2D Saint

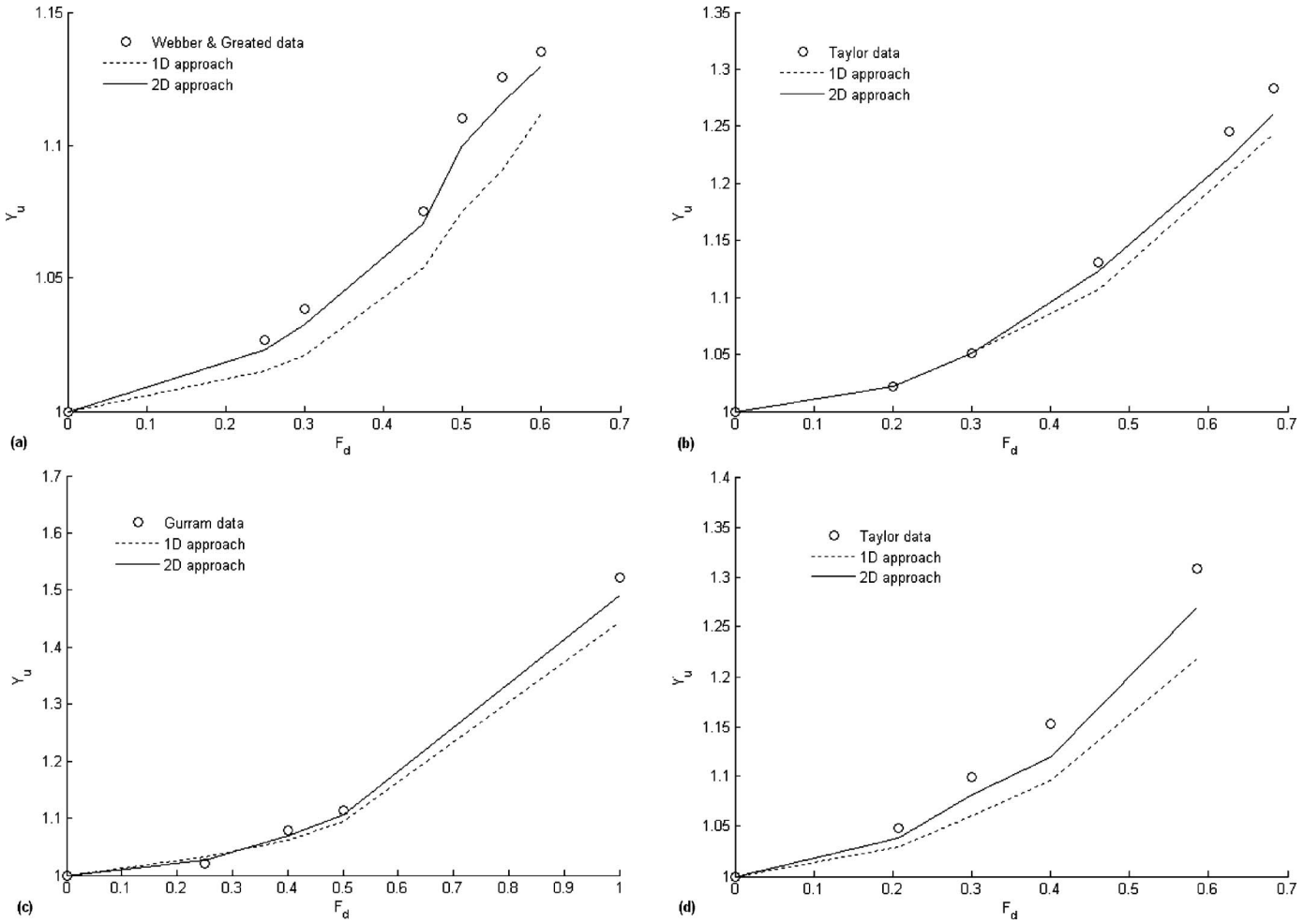

Fig. 5. Comparison of the main channel depth ratios with experimental data: (a) Webber and Greated (1966) data (angle=30° and q=0.2); (b) Taylor (1944) data (angle=45° and q=0.6); (c) Gurram (1994) data (angle=90° and q=0.25); and (d) Taylor (1944) data (angle=135° and q=0.8)

Venant equations are solved by a second-order finite-volume method with the Riemann solver of Roe (1981). The two approaches are compared to different experimental data. According to the comparison between the two approaches 1D and 2D and the experimental data of Taylor (1944), Webber and Greated (1966), Gurram (1994), and Hsu et al. (1998a,b), we can conclude that the 1D approach does not always achieve a very good agreement. This approach gives good results for small junction angle and small downstream Froude number. Once these parameters increase, the discrepancy between the 1D approach and the experimental data increases, while the 2D approach correlates well to the measured data and performs almost as well in all the considered cases and for the different flow parameters. This work shows therefore that the idea of combining a 1D approach in branches to a 2D approach for the junctions in practical situation is a good methodology when we observed the quality of the 2D simulation results. Therefore, future work will consist of developing a framework based on coupling:

- The 1D Saint Venant equations to be applied in branches; and
- The 2D Saint Venant equations to be applied at the junction area.

Notation

The following symbols are used in this technical note:

A = area of the control volume;
B = channel width;
c = wave celerity;
CFL = Courant number;
C_* = Chezy coefficient;
dt = time step;
E, G = flux vector;
E_Y = estimator of quality;
F = flux vector;
F = Froude number;
g = acceleration due to gravity;
h = water depth;
K = separation zone shear coefficient;
K^* = coefficient of interfacial shear;
L_i = length of interface between two control volumes;
n = unit vector outward to the boundary;
n_M = Manning's roughness coefficient;
Q = flow discharge;
q = discharge ratio;
R = Riemann invariant;
S = vector of source terms;
S_f = friction slope;
S_0 = bed slope;
S_0 = shear force on interface;
t = time;
U = vector of conserved variables;
u, v = velocity in the x and y directions;
w = width ratio;
x, y = Cartesian coordinates;
Y_u = upstream to downstream depth ratio;
Y_L = lateral to downstream depth ratio;
Γ = boundary of the control volume;
$\Delta\Gamma$ = length of the edge of a control volume; and
δ = junction angle.

Subscripts

d = downstream section in main channel;
L = downstream section in branch channel;
(L, R) = left and right sides of an edge; and
u = upstream section in main channel.

References

Akan, A. O., and Yen, B. C. (1981). "Diffusion wave flood routing in channel network." *J. Hydr. Div.*, 107(6), 719–723.

Best, J. L., and Reid, I. (1984). "Separation zone at open-channel junctions." *J. Hydraul. Eng.*, 110(11), 1588–1594.

Cockburn, B., and Shu, C. W. (1998). "The Runge-Kutta discontinuous Galerkin finite element method for conservation laws V: Multidimensional systems." *J. Comput. Phys.*, 141, 199–224.

Frazao, S. S., and Guinot, V.(2007). "An eigenvector-based linear reconstruction scheme for the shallow-water equations on two-dimentional instructured meshes." *Int. J. Numer. Methods Fluids*, 53(1), 23–55.

Garcia-Navarro, P., and Saviron, J. (1992). "McCormack's method for the numerical simulation of one-dimensional discontinuous unsteady open channel flow." *J. Hydraul. Res.*, 30, 95–105.

Gurram, S. K. (1994). "A study of subcritical and transitional combining flow in open channel junctions." Ph.D. thesis, Banaras Hindu Univ., Varanasi, India,.

Gurram, S. K., Karki, K. S., and Hager, W. H. (1997). "Subcritical junction flow." *J. Hydraul. Eng.*, 123(5), 447–455.

Hager, W. H. (1987). "Discussion of 'Separation zone at open-channel junctions,' by James. L. Best and Ian Reid." *J. Hydraul. Eng.*, 113(4), 539–543.

Hirsch, C. (1990). *Numerical computation of internal and external flows, computational methods for inviscid and viscous flows*, Vol. II, John Wiley & Sons, Chichester, England and New York

Hsu, C. C., Lee, W. J., and Chang, C. H. (1998a). "Subcritical open channel junction flow." *J. Hydraul. Eng.*, 124(8), 847–855.

Hsu, C. C., Wu, F. S., and Lee, W. J. (1998b). "Flow at 90° equal-width open-channel junction." *J. Hydraul. Eng.*, 124(2), 186–191.

Modi, P. N., Ariel, P. D., and Dandekar, M. M. (1981). "Conformal mapping for channel junction flow." *J. Hydr. Div.*, 107(12), 1713–1733.

Ramamurthy, A. S., Carballada, L. B., and Tran, D. M. (1988). "Combining open channel flow at right angled junctions." *J. Hydraul. Eng.*, 114(12), 1449–1460.

Roe, P. L. (1981). "Approximate Riemann solvers, parameter vectors, and difference schemes." *J. Comput. Phys.*, 43, 357–372.

Shabayek, S., Steffler, P., and Hicks, F. (2002). "Dynamic model for subcritical combining flows in channel junctions." *J. Hydraul. Eng.*, 128(9), 821–828.

Taylor, E. H. (1944). "Flow characteristics at rectangular open-channel junctions." *Trans. Am. Soc. Civ. Eng.*, 109, 893–912.

Webber, N. B., and Greated, C. A. (1966). "An investigation of flow behaviour at the junction of rectangular channels." *Proc., Institute Civil Engineers*, Vol. 34, London, pp. 321–334, 321–334.

Yen, B. C. (1979). *Unsteady flow mathematical modelling techniques: Modelling of rivers*, H. W. Shen, ed., Vol. 13, Wiley-Interscience, New York, 13–33.

Yen, B. C., and Osman, A. (1976). "Flood routing through river junctions." *ASCE Rivers'76*, Vol. 1, ASCE, New York, 212–231.